Journal of Fundamentals of Renewable Energy and Applications

Kumar et al., J Fundam Renewable Energy Appl 2017, 7:6
DOI: 10.4172/2090-4541.1000245

Research Article | Open Access

Optimization, Design, and Construction of Field Test Prototypes of Adaptive Hybrid Darrieus Turbine

Palanisamy Mohan Kumar[1,2]*, Subramani Anbazhagan[1], Narasimalu Srikanth[1] and Teik-Cheng Lim[2]

[1]*Energy Research Institute, Nanyang Technological University, Singapore*
[2]*School of Science and Technology, Singapore University of Social Sciences, Singapore*

Abstract

The current study presents the experimental optimization, design and construction of vertical axis Darrieus type micro wind turbine. Four turbines of different topology are fabricated representing the various operating configurations of novel adaptive Darrieus wind turbine developed to enhance the low wind speed performance of conventional straight bladed Giromill. As the Savonius rotor is integrated into Darrieus rotor, an optimized Savonius rotor diameter is achieved through wind tunnel test. The design, component selection and mechanical arrangement of scaled prototype intended for field test is discussed in detail. Gravity based tower is designed for the deployment of turbines and to withstand high wind conditions is presented along with structural analysis. The tower can be raised or lowered swiftly based on the wind conditions. Arduino platform based remote monitoring system is devised with web interface for data visualization and data storage. The study is intended to provide the design knowledge on small vertical axis micro wind turbines and shed additional light on sensor and data acquisition.

Keywords: Wind turbine; Darrieus; Low wind speed; Savonius; Adaptive

Introduction

Indiscriminate use of fossil fuels and their consequences on the mankind has raised a global concern and awareness on the use of renewable energy. Among various renewable sources wind energy is predominant with rapid annual growth rate of 35% for the past five years [1]. Small wind turbines are typically installed in locations of power requirement rather than at the optimum wind speed unlike large turbines. Darrieus wind turbines though efficient among vertical axis wind turbines, performs poorly in low wind speeds falling behind the horizontal axis counterparts. Past endeavors such as new airfoil design with trapped vortex [2] has elevated the performance level in low wind speed. Innovative design on airfoil such as NTU-20-V conceived to reduce the manufacturing cost of the straight blades [3] especially for urban installations, where the flow is highly turbulent [4]. Along with structural improvement, the performance improvement is evident through the computational comparative study [5] with conventional NACA 0018 airfoil. To enable Darrieus turbine capable of generating power at low wind speed without compromising the efficiency at high winds a novel Adaptive Darrieus Wind Turbine (ADWT) has been proposed. During operation, the ADWT adopts itself into different configurations based on the wind speed. The different configurations are created as individual turbines to study the starting characteristics and performance at high Tip Speed Ratio (TSR). The objective of the current study is to find the optimum Savonius rotor diameter through wind tunnel test and incorporate it field test prototypes. The critical factors that drives the design includes, but not limited are reliability, ease of maintenance, low cost, no wake interference between rotors, simple power transmission and inexpensive towers that can be raised and lowered without external power assistance. A static structural analysis on the tower elements and the foundation structure is carried out to ensure the safe operation. A concrete free foundation is preferred as study is for short duration and not a permanent installation. The rotor rpm, generator output and the wind speed of four turbines are measured for comparison and assessing the performance. The subsequent sections describe the process of achieving the above said objectives subjected to the constraints towards the design of four turbines.

Materials and Methods

Working principle of adaptive darrieus wind turbine (ADWT)

The two critical challenges the Darrieus turbine is facing today are the poor performance at low wind speed and over speed regulation. These imperative problems require immediate attention and implementable solution. The previous attempts do yield solutions, but the complexity and the cost limits its application in commercial turbines. The solution for these challenges should be developed with the boundary conditions such as low cost, increased starting torque at low wind speed and able to sustain the rotation, able to control the rotational speed if the rotor spins beyond the rated rpm. The airfoil at low Reynolds number inherently develops low lift [6]. The decrease in the lift is further exacerbated by the high Angle of Attack (AoA) [7]. The inadequate lift is not sufficient to generate the torque that can overcome the inertial and drive train resistance [8] and thus failing to incite the rotation at low wind speeds. Generating torque only by lift force at low wind speed is not pragmatic for a Darrieus turbine and past studies bolster the above statement with wind tunnel experiments and field test [9]. To circumvent the problem of low lift, considerable drag force can be employed to generate the torque even at low wind speed such as Savonius rotor. The Savonius rotor creates drag and converts into torque in which the magnitude depends on the difference between the drag force of concave and convex portion of the blade [10]. The Savonius rotor excels in performance than the Darrieus turbine in weak wind flows. Hence a hybrid turbine will be appropriate, but the reduction of power coefficient at high TSR is inevitable as indicated

***Corresponding author:** Palanisamy Mohan Kumar, Energy Research Institute, Nanyang Technological University, 50 Nanyang Ave, Singapore, Tel: +65 6791 1744; E-mail: pmkumar@ntu.edu.sg

Received November 09, 2017; **Accepted** November 19, 2017; **Published** November 27, 2017

Citation: Kumar PM, Anbazhagan S, Srikanth N, Lim TC (2017) Optimization, Design, and Construction of Field Test Prototypes of Adaptive Hybrid Darrieus Turbine. J Fundam Renewable Energy 7: 245. doi: 10.4172/2090-4541.1000245

Citation: Kumar PM, Anbazhagan S, Srikanth N, Lim TC (2017) Optimization, Design, and Construction of Field Test Prototypes of Adaptive Hybrid Darrieus Turbine. J Fundam Renewable Energy 7: 245. doi: 10.4172/2090-4541.1000245

by the past studies [11]. Hence the proposed solutions to avert the influence of Savonius rotor at high wind speed are:

- Disengage the Savonius rotor from the Darrieus rotor shaft when the TSR is greater than 1 [12]. This solution is feasible when the Savonius rotors are placed outside the Darrieus rotor, in which the wake generated by the Savonius rotor will not impact the Darrieus rotor. This solution may not be applicable for higher kW capacity as the main shaft length will be doubled with negative impact on structural properties.

- By using a telescopic Savonius turbine to retreat the buckets into a cylinder and reducing the drag torque of the Savonius rotor.

- By converting the two bladed Savonius rotor into a cylinder with minimum wake on the downstream. This concept is feasible than the above said options which affects the aerodynamic and structural aspects considerably. Added advantage is that this concept is able to regulate the rotor overspeed which lacks in the above-mentioned options.

Based on the above discussion, the Darrieus rotor can be well integrated with two stage Savonius rotor with two buckets on each stage. The Savonius buckets can slide perpendicular to the axis of rotation, there by varying the torque generation both in magnitude and direction. Since the turbine can adopt itself to the wind conditions, it is referred as Adaptive Darrieus Wind Turbine (ADWT). ADWT basically operates in three configurations as shown in the Figures 1a-1c. During low wind speed, the Savonius rotor and the Darrieus rotor can generate torque in the same direction up to TSR 1 as shown in Figure 1a. When the hybrid rotor reaches TSR 1 with respect to Savonius buckets, they can slide to form a cylinder giving rise to a minimum wake that has less impact on the downstream of the Darrieus rotor as shown in Figure 1b. At high wind speeds when the rotor reaches its rated rpm, the configuration as shown in Figure 1c will be deployed, in which the Savonius buckets slide away from the axis to create torque opposing the Darrieus torque. Eventually the hybrid rotor will decelerate in speed and the rotor can be parked by dynamically adjusting the distance between the Savonius bucket to the axis (Figure 1).

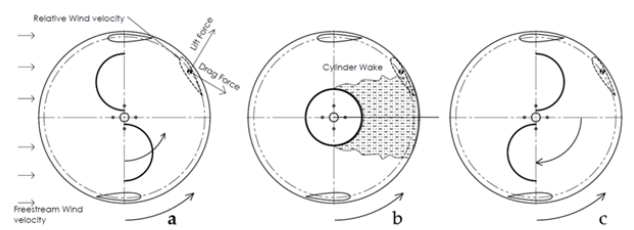

Figure 1: Various configurations of Adaptive Darrieus Wind Turbine (ADWT).

Figure 2: ADWT under wind tunnel test (left) and various diameters under investigation (right).

Experimental Optimization of High Solidity ADWT

Wind tunnel setup and models

An experimental optimization is carried out in search of optimum Savonius diameter on a straight bladed Darrieus turbine through wind tunnel test. Though it is desirable to have a larger Savonius rotor for better starting characteristics, the closed rotor configuration (cylinder) will curtail the power performance of Darrieus turbine. Hence an optimum diameter exists at which the reduction in power coefficient is at acceptable. ADWT under wind tunnel test (left) and various diameters under investigation (right) level and that's where the wind tunnel test is headed on. Various diameter Savonius rotor in closed configuration is tested for different wind speed and the performance of Darrieus turbine is recorded. An optimum diameter range will be evident from the results. The diameter chosen for the wind tunnel investigation are 20, 40, 80, 100, 150, 200 mm as shown in Figure 2 and they are integrated with 400 mm diameter straight bladed Darrieus turbine. Since the optimization is to enhance the low wind speed performance of Darrieus turbine, three blades of NACA 0021 airfoil is chosen. The blades are arranged between the top and bottom end plates made of acrylic. The airfoil and the cylinders were made by 3D printing through Fused Deposition Moulding (FDM). The cylinders are made in two halves to interchange without disturbing the Darrieus rotor airfoils and the main shaft alignment. The fabricated prototype is subjected to varying wind speed from 5 m/s to 9 m/s in ERIAN subsonic wind tunnel. The wind tunnel can generate maximum wind velocity of 12 m/s by 0.9 m diameter axial fan (Multi-Wing). The speed of the fan can be varied through variable frequency drive. The turbine shaft is positioned by deep groove ball bearings on bottom and spherical roller bearing on top. The main shaft is connected to the torque sensor through flexible coupling. The other end of the torque sensor is connected to magnetic particle brake (Placid Industries) to apply brake torque by varying the DC power supply. The rpm is measured by proximity sensor and hot wire anemometer (Kanomax) is employed to measure the wind speed in the test section. Since the rotor occupies 36% of test section frontal area, the freestream wind speed v_f are blockage corrected v_c as suggested by [13] given by the Equation (1) and Equation (2),

$$B_T = \frac{Model\ Frontal\ Area}{Test\ Section\ Area} \tag{1}$$

$$v_c = v_f\left(1 + B_T\right) \tag{2}$$

Results and Discussion

Torque, rpm, and corresponding wind speed are recorded for the different diameters under investigation and the data is condensed to calculate the power coefficient C_p from the rotor torque T and the measured angular velocity ω as per the below mentioned equations.

$$C_p = \frac{P_{rotor}}{P_{wind}} \tag{3}$$

$$P_{wind} = 0.5 * \rho * A_s * V_c^3 \tag{4}$$

$$P_{rotor} = T * \omega \tag{5}$$

The ADWT is subjected to the wind speed of 5, 6, 7, 8 and 9 m/s corresponding to the airfoil Reynolds number of (Re) 1.4×10^5, 2.3×10^5, 2.6×10^5, 2.8×10^5. The Darrieus rotor performance under the influence of varying diameter is recorded to determine the maximum diameter of the Savonius rotor in ADWT. The wind flow on the Darrieus turbine by itself is complicated due to varying AoA and varying wind velocity on its path along the azimuthal position, which is further compounded by the interactions of wake from the cylinder on the Darrieus turbine airfoil. Hence a profound knowledge on the wake behind the cylinder at the investigated wind speed is indispensable. For the wind speed spectrum and the diameter range, the Re over the cylinder is in the range of 7000 to 120,000 which is different from the airfoil Re stated above. Diameter based Re has been singled out as the influential parameter on the aerodynamics of cylinder. The dispersion nature of wake and the wake width on the airfoil flight path is the deciding factor of Darrieus rotor performance and it is apparent that, a minimum wake width will have minimal impact. The flow characteristic over cylinder in this regime is subcritical and flow pattern is periodic with the formation of eddies in a sinusoidal manner giving rise to wake instability as shown in Figure 3. The flow is fully turbulent with vortex shedding at specific frequency based on the Strouhal number. The above said phenomenon is based the studies that the incoming flow is laminar and the cylinder is not rotating. Whereas in the current case, the incoming flow itself is highly turbulent wake from the upstream of the Darrieus rotor and cylinder is rotating and hence it is impervious to understand the flow physics in this complex environment. Drag coefficient of the cylinder varies according to the Re. Hence the experimental results of the Darrieus rotor performance will shed light on the optimum diameter range of cylinder from where the Savonius rotor can be constructed. For 5 and 6 m/s low wind speed, the 20 mm diameter dominates in performance and of course 200 mm diameter displays the least performance. The flow in this regime over the cylinder is laminar and disturbance from the cylinder is minimal. At 5 m/s the of the C_p 20 mm cylinder is 0.10 at TSR 1.35 after which the *Cp* starts to decline, whereas the larger diameters tend to reach their peak power coefficient at higher TSR above 1.4. For he tested wind speed the maximum *Cp* of all the diameters are clustered around TSR 1.4. At all other wind speeds, the 100 mm cylinder outperforms other diameters. The higher *Cp* can be attributed to the skewed flow from the cylinder which is directed to the certain azimuthal position, where the blade is able to generate higher lift due to favorable AoA and higher relative wind velocity contributing to the total torque. The corresponding Re of the cylinder at 6 m/s is 112, 621 at which the flow over the cylinder starts to form numerous secondary vortices. It can be generalized that the flow is shifted aft the axis of the cylinder leading to an increase in the flow velocity due to rotation. The increased performance of 100 mm cylinder than the smaller diameters leads to a valuable conclusion. The closed Savonius rotor is similar to the center shaft in a conventional Darrieus turbine. The assumption of researchers and designers of Darrieus turbine is far is that the center shaft diameter is inversely proportional to the Darrieus performance. But the experimental results contradict the above statement not only for a specific wind speed, but for most of the wind speeds. This indicates that there exists an optimum diameter that increases the *Cp* of the Darrieus turbine. The positive effect of larger diameter influences the structural characteristics significantly. A thin walled larger diameter shaft is desirable for the structural rigidity and for reduced vibrations (Figure 4).

When comparing the Cp of 100 mm and 20 mm, 100 mm cylinder is 26.6% less at 5 m/s, 12.3% less at 6 m/s, 3.7% more at 7 m/s and 2.7% more at 8 m/s. Furthermore the 100 mm cylinder operates at a wider TSR than other diameters, considerably outputting more annual energy as the turbine can operate in a wider wind sped spectrum. At 8 m/s, the differences between peak power coefficients of all the diameters are closer except 200 mm. The least performance of 200 mm is due to the influence of oncoming wind in the upstream of Darrieus rotor, whereas other diameters influence only on the downstream. The results are plotted with TSR against C_p for different diameter for each wind speed as shown in the Figures 4 and 5.

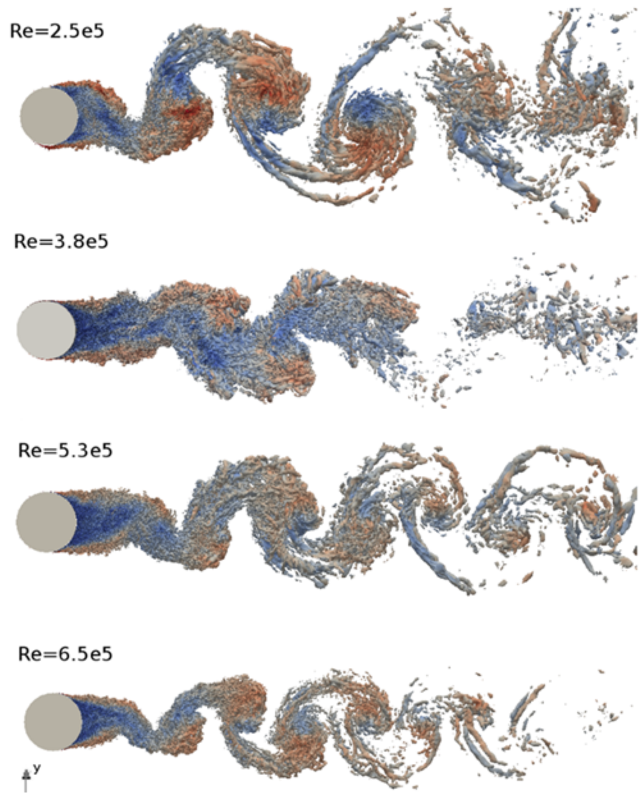

Figure 3: Typical flow characteristics over a cylinder.

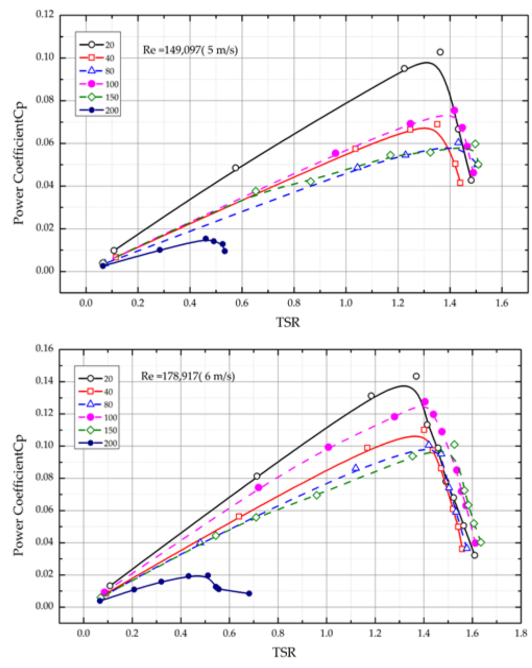

Figure 4: Power coefficient vs. tip speed ratio at 5 m/s (top) and 6 m/s (bottom).

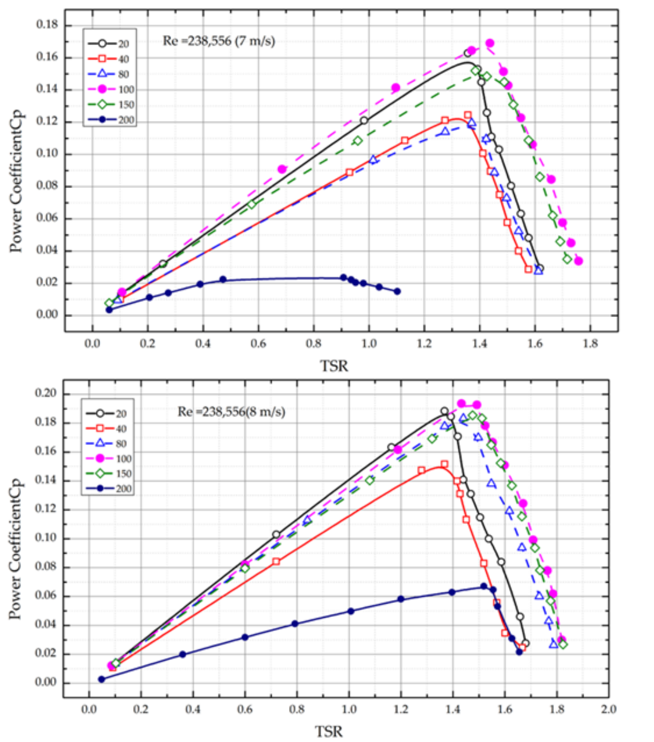

Figure 5: Power coefficient vs. tip speed ratio at 7 m/s (top) and 8 m/s (middle) and 9 m/s (bottom).

Description of the Field Prototypes

Field test configurations

The field prototypes are to be deployed in the field to monitor the performance under natural flow characterized by low and fluctuating flows. The field test configurations are shown in the Figure 6.

Darrieus rotor

The airfoil characteristics have profound effect on the Darrieus turbine performance. Since the current study is not about the optimization and merely a comparative study, the airfoil profile may not have a significant role. The desirable property of an airfoil for micro turbine is to generate higher torque at most of the azimuthal position that can overcome the resistive torque to start rotating. Hence a cambered airfoil is preferred than symmetrical airfoils [14]. The past experimental study indicates that the annual energy output does not decrease significantly for a symmetrical and cambered airfoil. Since the cambered airfoil has the advantage of early start and able to generate power at low wind speed, a cambered airfoil with sufficient thickness is opted for the current study. The airfoil SH3055 is a low Reynolds number airfoil with thickness of 18% at 38% chord (c) and mean camber of 7% at 12% with the chord length of 120 mm. The chosen airfoil profile along with the conventional NACA0018 has been described below. To generate higher torque at low wind speed more number of blades is preferred [15]. In other words, the increased solidity will bolster the low wind speed performance. Furthermore, increase in the number of blades increases starting torque and the directional starting in relation to the oncoming wind. Four blades are chosen as number of blades more than five will deteriorate the efficiency due to the blade

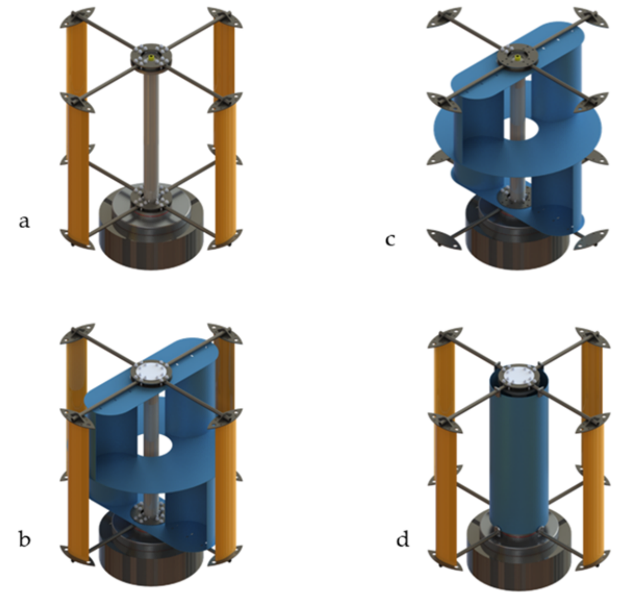

Figure 6: (a) Conventional darrieus (b) Darrieus with savonius in open configuration (c) Conventional savonius (d) Darrieus with savonius in closed configuration.

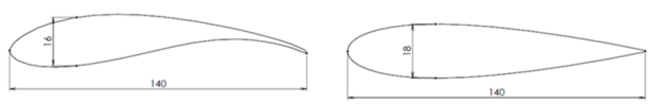

(a) (b)

Figure 7: (a) SH3055 airfoil and (b) NACA 0018 airfoil.

wake interaction. Blades are manufactured from glass fiber material by moulding process. Thread inserts are placed inside the blades during moulding to facilitate the attachment with the structs (Figure 7).

Savonius rotor

The Savonius buckets of optimum diameter in open condition (Semicircular profile) and closed condition (cylindrical profile) are fabricated from 2 mm aluminum sheet. The fabricated buckets and the cylinder are shown in Figure 7. The Savonius buckets are mounted on the struct fixing flange. The Savonius bucket in open configuration has additional circular ribs to prevent it from deformation at high winds. It is conventional to equip Savonius rotor with endplates for structural rigidity and to prevent the air flowing over the rotor, the current rotor is devoid of end plates to simulate a larger rotor when scaled to higher capacity turbines [16].

Struts

Struts are members that connects the blade to the main shaft. The primary function of the struct is to support the blades, withstand the centrifugal force and to prevent the blades from vibration. In addition, these primary functions are to be met at lowest drag based. The previous studies on the struct shed light on their influence on the turbine performance. The drag caused by the structs are significant especially near the rotor periphery due to high tip speed. It was found that the struts decrease the annual energy production by 26% compared to the turbine without struts [16]. To keep the strut drag to minimum and to curtail the cost, a cylindrical profile was chosen. The mild steel pipe is welded to the flange to connect to the rotor shaft on the inner part and on the outer part is to fix the blades. The completed struct is shown in Figure 8.

Generator

Each configuration is equipped with 100 watts permanent magnet generator manufactured by Wuxi Fend Tech. The generator chosen has low cogging torque to enable the rotor to start at low wind speed. The output from the generator is three phase variable frequency AC power rated at 800 rpm to deliver 100 watts. The generator shaft has male thread of M16 × 1.5 to connect with the rotor main shaft (Figure 9).

Controller

The MPPT based controller is employed to allow the turbine to operate at its maximum efficiency. The controller model is FW02-24 as shown in Figure 9b. The controller receives the variable frequency AC input from the generator and converts into 24V DC. The MPPT algorithm defines the efficient operating point for the given rotor rpm and the wind speed. Controller is able to handle a maximum power of 600 watts with IP67protectciton to deploy in the field. The controller can apply electrical brake through the generator by short circuit the three power leads to protect the turbine from over speeding.

Power transmission

The design of the power transmission system is based on the constraints such as low cost, ease of assembly, step up the rotor rpm to match the rated rpm of the generator and able to accommodate in the given space. The conventional power transmission is to fix the rotor shaft directly to the generator in which case a large generator with higher number of poles are required to deliver the rated power. Increasing the poles significantly increases the cost, size and weight of the generator as the rotor rpm is low. Another sophisticated way is to incorporate the gear train to step up the speed together with high rpm small sized generator. The gear train undoubtedly generates noise and requires periodic maintenance. To avert the above said issues a novel friction drive has been employed in the current design. The rotor is connected to the cylindrical aluminum disc of diameter 300 mm and the generator shaft is fixed with elastomeric wheel of diameter 75 mm achieving a step-up ratio of 1:4 as shown in Figures 9a and 9b. The generator is

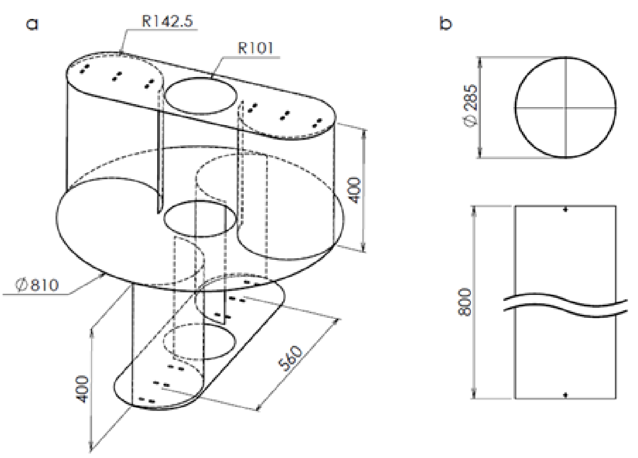

Figure 8: (a) Savonius rotor dimensions in open configuration (b) Savonius rotor in closed configuration.

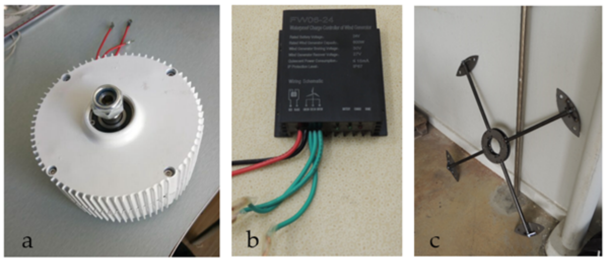

Figure 9: (a) Generator (b) Controller (c) Manufactured structure.

fixed on the slide plate guided by the slots and preloaded with the spring to ensure that sufficient normal force is applied to the wheel to create enough friction and to prevent slippage. The power transmission depends on the contact force, transmission ratio, rotational speed, and coefficient of friction. For a material combination in which one of the two materials is an elastomer, a coefficient of friction $\mu=0.7$ can be applied and together with spring force to vary the friction between the surfaces can be varied (Figure 10).

The friction drive has notable merits over conventional gearbox by eliminating bearings and oil that demands periodic filtration and replacement. The overall manufacturing and maintenance cost will be reduced. Moreover, energy from gusts is stored as momentum in the flywheel which will smoothen out the torque pulsation generated by the Darrieus rotor.

Main shaft and rotating shaft

The main shaft is a non-rotating member made of 30 mm mild steel hollow shaft of wall thickens 3 mm as shown in Figure 10a with the completed Darrieus rotor (Figure 10b). The main shaft flange is fixed to the tower flange and supports the ball bearings separated by spacer of length 600 mm arrested axially by circlips. The rotating shaft is mounted on bearings with the flanges welded on top and bottom to fix the struts brackets. The rotating shaft is 50.6 mm in diameter with the wall thickness of 2.5 mm (Figure 11).

Tower Design

Wind turbine tower

The conventional tower design for micro turbines with power capacity less than 2 KW are either guy wired tower erected with gin pole or monopole tower fixed on the concrete foundation. The monopole towers can be either hydraulically erected or permanently fixed on the foundation. Compared to monopole towers guy wired towers are inexpensive especially for small turbines. The guy wired towers consists of the mild steel pipe of 101.6 mm in diameter and 8 m height hinged to the foundation plate. The gin pole is welded perpendicular to the main tower of height 2 m. The steel rope that passes through the gin pole has to be pulled in order to erect the turbine. In the current design, the pulling force is provided by manual winch with maximum pull force of 2000 kg (Model No: Fuji PNW-2000). The critical components are identified in Figure 11.

Two vital factors that should be considered in designing a tower that supports the wind turbine are the deflection at maximum load and the excitation frequency. Apart from the gravity loads on the tower, the thrust is significant and may be even higher. As per IEC 61400-2, the maximum thrust load is generated when the turbine is subjected to 50 years extreme wind speed when in parked condition or faulty wind

Citation: Kumar PM, Anbazhagan S, Srikanth N, Lim TC (2017) Optimization, Design, and Construction of Field Test Prototypes of Adaptive Hybrid Darrieus Turbine. J Fundam Renewable Energy 7: 245. doi: 10.4172/2090-4541.1000245

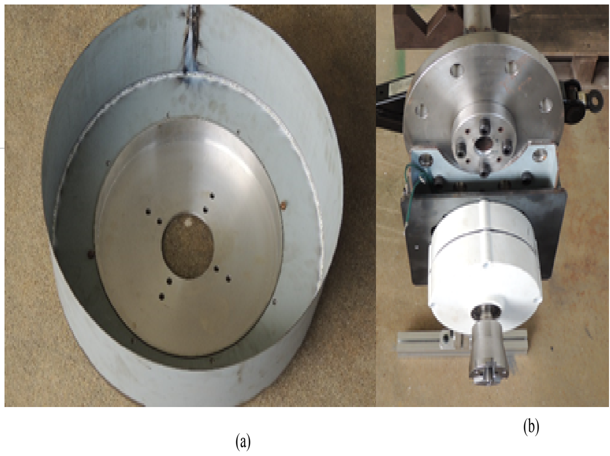

Figure 10: (a) Friction disk and (b) Generator with elastomeric wheel adaptor.

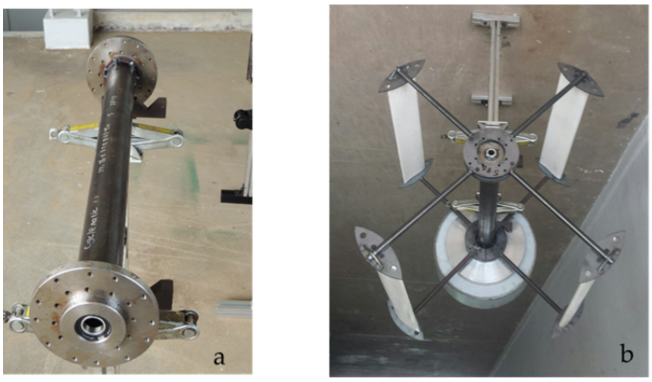

Figure 11: (a) Main shaft (b) Fabricated darrieus turbine.

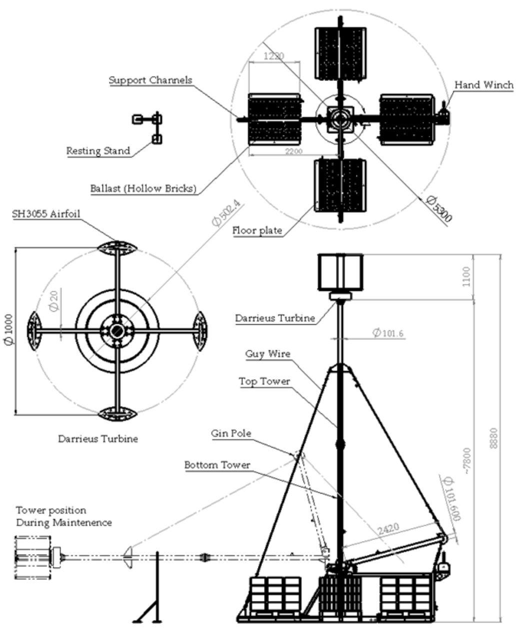

Figure 12: Wind turbine tower dimensions.

turbine under no load or brake. Maximum thrust load of 1960 N is calculated as stated by IED codes and nacelle load of 200 kg is applied on the turbine tower in X and Z direction as shown in Figures 12a and 12b. The results show that with ASTM A36 material of yield strength 370 MPa, the maximum stress developed in the top tower and turbine fixing flange are 138 MPa and 99 MPa respectively yielding a 2.68 as factor of safety for tower. The maximum tower deflection is 59 mm, which is far less than allowable 1% deflection as shown in Figure 12c. The tower is subjected to frequency extraction. Considering 3.33 Hz and 5 Hz corresponding to the rotor rpm of 220 at rated wind speed and 300 as maximum rotor speeds, the first mode of tower frequency is 2.5 Hz as shown in Figure 12d. Key support structures such as ballast channel and the gin pole are analyzed for deflection and buckling respectively as illustrated in Figures 12e and 12d respectively. The maximum deflection on the loading direction of the channel is recorded as 19.3 mm and maximum stress is 120 Mpa. The critical load to buckle the gin pole is 1.2×10^5, whereas the applied load is only 2670 N. The installed turbine tower is depicted in Figure 12b.

Sensor tower

The wind vane and the anemometer are mounted on a dedicated tower independent of the turbine towers. The tower apart from holding wind measurement sensors protects the turbines and the sensors from lighting. Singapore is one of the places with highest number of lightings per year and it is mandatory to install lighting poles on tall structures. The sensor tower is 10 m height and uniquely designed for easy maintenance. The tower has a mid-hinge that can fold down with hand operated cable and in similar way can be folded up. The anemometer and the wind vane are to be mounted on the top plate at a distance of 2 m in-between to avoid any flow disturbances due to tower. Though the tower top loads are negligible, a hexagonal shaped tower will avoid any vortex shedding that induces vibrations as in the case of a circular tower. The installed anemometer tower is shown in Figure 13.

Foundation Design

Gravity foundation for wind turbine

The duration of the comparative study is short and hence a permanent concrete foundation is not economical and cannot be relocated as and when needed. An appropriate foundation should be inexpensive and able to relocate. A gravity based foundation is pragmatic in curbing the installation cost of the foundation by $1/3^{rd}$ of the conventional concrete foundation cost. The gravity tower can be rapidly installed and decommissioned while occupying smaller foot print. In addition, the gravity foundation eliminates the need for larger cranes as the only heaviest part is the ballast. Instead of a single concrete block, the ballast is made of individual hollow bricks that can be handled manually. The gravity tower is surface coated (galvanized) to prevent any corrosion as they are installed in the vicinity of sea. A low cost galvanized steel pallet holds the ballast in place and fixed to the foundation structure and thus transmitting the load safely to the ground. Four crates are provided and each crate holds 1000 kg of ballast weight creating an opposing moment of 15 kNm from the tower axis. The installed gravity foundation for the wind turbine is presented in Figure 14.

Gravity foundation for sensor tower

The sensor tower gravity foundation is designed in a similar way as the wind turbine tower foundation. Since the thrust load on the tower top is negligible compared to the wind turbine tower, the support structures can be of simple design and the ballast weight can be reduced

Figure 13: (a) Installed anemometer tower and (b) Installed wind turbine tower.

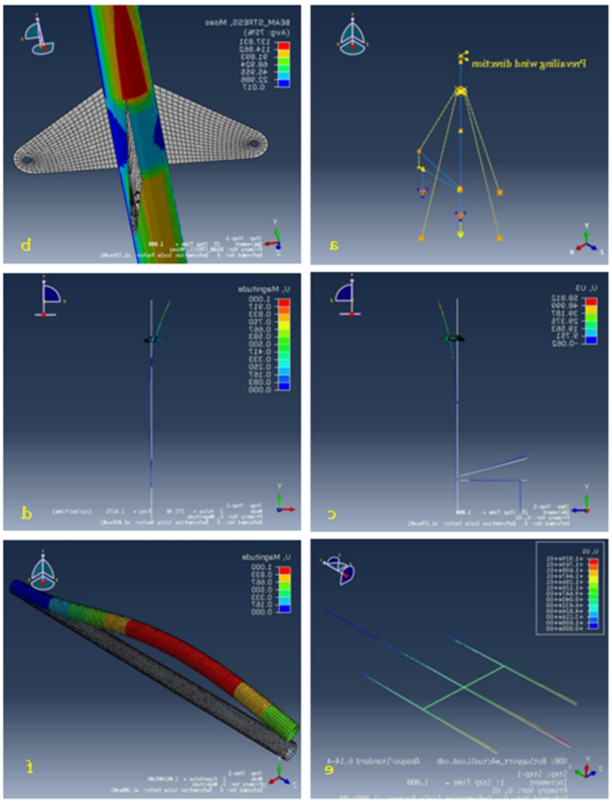

Figure 14: Structural analysis and frequency analysis of various components of wind turbine tower.

to 600 kg on each arm. The support structures are made with standard structural shapes to reduce the cost of manufacturing. Scaffolding planks are employed to distribute the ballast weight to a larger area on the ground. The installed gravity foundation for the sensor tower is presented in Figure 15.

Sensing and Data Logging

An accurate mode on sensing at specific intervals is vital for assessing the turbine performance. A set of sensors that are highly reliable and repeatable are chosen for the current study. The parameters of interest are rotor rpm, generated voltage, current, wind speed and wind direction. As the turbines are to be monitored at real time, the data from the four turbines must be logged concurrently, which induces a bit of complexity compared to logging data from a single turbine. Since the turbines are located at 20 m apart, interconnecting with data acquisition system by cables is not economical. Hence inexpensive wireless transmission will be appropriate for the short-range data transfer. Though a variety of wireless protocols are available, a well-established and inexpensive ZigBee protocol will be opt for the current study. The data acquired from various sensors are transmitted through IoT gateway and real-time monitoring is enabled through a web interface. The following sections explain in detail about the sensing elements and the wireless transmission network.

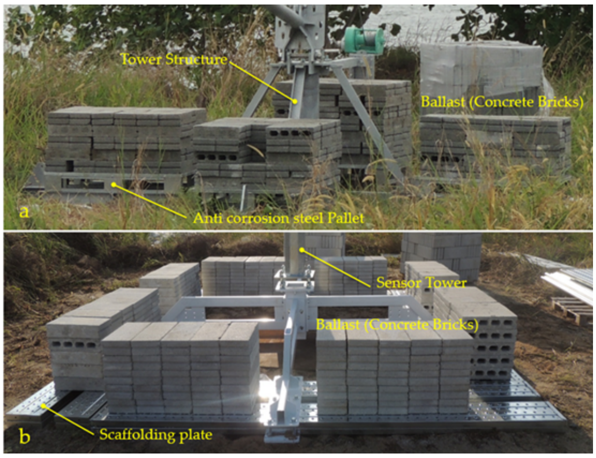

Figure 15: (a) Installed wind turbine tower gravity foundation (b) Installed anemometer gravity foundation.

RPM sensor

The rotational speed of the rotor is an essential parameter in determining the mechanical energy that is extracted from the wind, to calculate TSR for insight on aerodynamic characteristics, to compute aero loads for structural optimization. Since the rpm measurement can be made in various methods and sensors, an inexpensive and reliable way is to use an inductive proximity sensor (Model no: XMS-20). The proximity sensor outputs 4-20 mA current pulse when it detects a ferrous object in the vicinity. The generated pulses are counted for 60 s that corresponds to the rotor rpm. Added advantage of employing proximity sensor is the minimum space requirement and IP 67 protection to install in outdoor conditions.

Micro controller

A microcontroller can be employed for data gathering and for condition based actuation, for instance to disengage the load to prevent the battery from deep discharge. Arduino Uno is a simple controller with open platform programming employed in the present study. The maximum analog input voltage for Arduino is 0-5 V DC, hence the output from various sensors are to be converted to 0-5 V DC to directly plug in. Thanks to low cost Arduino shield that performs the conversion job and enables a seamless integration of various sensors. Arduino has to be supplied with 9 V DC power supply independent of the turbine output. A solar panel with battery will ensure an uninterruptable power supply. The sampling rate of the measurements is for every 5 minutes

Voltage and current measurement

A simple voltage divider circuit is used to convert the full range 0-380 V to 0-5 V DC. The measured rms voltage is then fed into Arduino for further transmission. A much more convenient way is to use the voltage transducer that can output 0-5 V DC. A current transducer finds its place around the power line from the generator. The Arduino based current transducer outputs 4-20 mA in proportional to the incoming ampere. The chosen Model is CMN 20 and it is able to measure up to 72 A with the response time of 250 s.

Power measurement

In order to determine the power coefficient (C_p) or efficiency of the turbine, the power available in the wind and the power output by the generator has to be computed. The Equation 4 will output the wind power from the measured wind speed. The power output from the generator is measured from the voltage and the current transducer as per the Equation 8.

$$P_{rotor} = V_{rms}\, x\, I_{rms} \quad (6)$$

The following table provides the sensor, purpose, and the output (Table 1).

Sensor	Sensing Parameter	Output
Proximity Sensor	Rotor rpm	4-20 mA
Voltage sensor	Generated Voltage	0-5 V DC
Current sensor	Generated Current	4-20 mA
Anemometer	Wind speed	0-5 V DC
Wind Vane	Wind Direction	0-5 V DC

Table 1: Sensors and their purpose.

ZigBee wireless transmission and web interface

As quoted earlier, the turbines are placed at 20 m apart and necessitate ZigBee based wireless protocol adoption for the current study. ZigBee is developed by ZigBee alliance defined by IEEE 802.15.4 standard and has been successfully used on several remote monitoring applications. Added advantage is their compatibility with Arduino. Since for the current layout of the turbine is 100 m the ZigBee model X37-24-C is selected that has the transmission distance of 150 m and can be further increased by extending the antenna length. Both the transmitter and the receiver operates at 2.4 GHz frequency range. The Arduino in the sensor tower acts as the coordinator forming the network with IoT gateway and other ZigBee modules mounted on the Arduino of four turbines. The overall system architecture including the data transmission system is shown in Figure 15. The web interface includes real time data visualization and geographical map interface with the details of location coordinates sensed by GPS. The webpage is developed through HTML with the feature to include the additional turbine parameters if needed.

Conclusion

A wind tunnel optimization on ADWT has been carried out with different diameter of Savonius rotor in closed configuration. Albeit a smaller diameter has less impact on the Darrieus performance, a maximum possible diameter is favorable for low wind speed performance. Maximum Cp of 0.19 is reported for 100 mm shaft at 8 m/s and the Cp reduces by 4.2% for 150 mm, 65.1% for 200 mm for the wind speed of 8 m/s. At low wind speed of 5 m/s, the Darrieus turbines shows a performance coefficient of 0.068 with 40 mm shaft. For most of the wind speed, the 150 mm and 200 mm diameter displays poor performance and the reason is obvious that, bigger diameter cylinder generates larger wake width reducing the lift at specific azimuthal position of the blades. The diameter range of 100 mm to 150 mm shows an acceptable reduction in power coefficient. Hence the optimum diameter with improved starting characteristics and minimum impact on the performance of Darrieus turbine is 120 ± 10 mm. With this optimum diameter from the wind tunnel test, field prototypes of rotor diameter 1000 mm are designed. The critical components such as tower and the supporting structures are subjected to structural analysis to ensure the deflection is under allowable limit. The natural frequency and modes are investigated to avoid resonance with blade passing frequency. The sensing elements compatible with Arduino were selected and wireless transmission network is created to log the data from the four turbines. Future work is to scale the optimum configuration to 10 kW and compare the performance with conventional turbines available in the market (Figure 16).

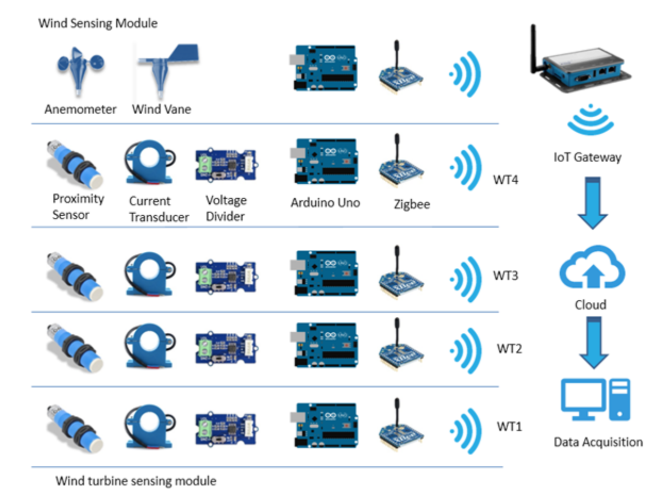

Figure 16: Wireless transmission network with selected sensors.

Acknowledgements

This research was supported by the National Research Foundation, Prime Minister's Office, Singapore under its Energy Innovation Research Programme (EIRP Award No. NRF2013EWT-EIRP003-032: Efficient Low Flow Wind Turbine).

References

1. Savino MM, Manzini R, Selva VD, Accorsi R (2017) A new model for environmental and economic evaluation of renewable energy systems: The case of wind turbines. Applied Energy 189: 739-752.
2. Kumar PM, Surya MM, Srikanth N (2017) On the improvement of starting torque of Darrieus wind turbine with trapped vortex airfoil. 2017 IEEE International Conference on Smart Grid and Smart Cities (ICSGSC).
3. Kumar PM, Surya MR, Sin NP, Srikanth N (2017) Design and experimental investigation of airfoil for extruded blades. International Journal of Advances in Agricultural and Environmental Engineering 3: 395-400.
4. Karthikeya B, Negi PS, Srikanth N (2016) Wind resource assessment for urban renewable energy application in Singapore. Renewable Energy 87: 403-414.
5. Kumar PM, Surya MM, Srikanth N (2017) Comparitive CFD analysis of Darrieus wind turbine with NTU-20-V and NACA0018 airfoils. IEEE International Conference on Smart Grid and Smart Cities (ICSGSC).
6. Mangalam S, Pfenninger W (1984) Wind-tunnel tests on a high performance low-Reynolds number airfoil. 13th Aerodynamic Testing Conference.
7. Shigemi M (1993) Numerically simulated flow separation on airfoil of high angle of attack. Fluid Dynamics of High Angle of Attack, pp: 109-120.
8. Bati A, Luk P (2015) Analysis of drive-train resonance and torque ripple smoothing of a 50kW vertical axis wind turbine. IEEE International Conference

on Industrial Technology (ICIT).

9. Ai D (1979) Low cost Darrieus vertical-axis wind turbine design. Terrestrial Energy Systems Conference.

10. Dobrev I, Massouh F (2011) CFD and PIV investigation of unsteady flow through Savonius wind turbine. Energy Procedia 6: 711-720.

11. Chawla S, Chauhan A, Bala S (2015) Parametric study of hybrid Savonius-Darrieus turbine. 2nd International Conference on Recent Advances in Engineering & Computational Sciences (RAECS).

12. Baz AM, Mahmoud NA, Hamed AM, Youssef KM (2015) Optimization of two and three rotor savonius wind turbine. Oil and Gas Applications; Supercritical CO2 Power Cycles; Wind Energy.

13. Rae A, Pope WH (1999) Low speed wind tunnel testing (3rd edn.). John Wiley & Sons, Ltd. New York.

14. Lassig J, Sosa JV, Jara U (2016) Wind tunnel testing of a small wind turbine Darrieus-H, with asymmetric airfoil, for auto start. IOSR Journal of Mechanical and Civil Engineering 13: 63-69.

15. Sunyoto A, Wenehenubun F, Sutanto H (2013) The effect of number of blades on the performance of H-Darrieus type wind turbine. International Conference on QiR.

16. Paraschivoiu I, Fraunie P, Beguier C (1985) Stream tube expansion effects on the Darrieus wind turbine. J Propul Pow 1: 150-155.